DOI: 10.1143/JPSJ.80.084201

Screening Potential of ^{6}Li(d,α)^{4}He and ^{7}Li(p,α)^{4}He Reactions in Liquid Lithium

Kaihong FANG[1,2*], Tieshan WANG[1], Hiroki YONEMURA[2†], Akinori NAKAGAWA[2‡], Takahiro SUGAWARA[2§], and Jirohta KASAGI[1,2]

[1]*School of Nuclear Science and Technology, Lanzhou University, Lanzhou, Gansu Province 730000, P. R. China*
[2]*Laboratory of Nuclear Science, Tohoku University, Sendai 982-0826, Japan*

(Received February 23, 2011; accepted May 19, 2011; published online August 10, 2011)

In order to investigate the screening effect of a nuclear reaction in a liquid metal environment, thick-target yields of the ^{6}Li(d,α)^{4}He and ^{7}Li(p,α)^{4}He reactions were measured using a liquid Li target for incident energies between 22.5 and 70 keV. The modified $S(E)$ factor [$S^{*}(E)$] for the liquid Li environment was deduced by dividing the measured yield by the energy integration of the penetration factor divided by the stopping power. It was shown that $S^{*}(E)$ for the liquid environment is considerably larger than that for the atomic/molecular environment for both reactions. The difference in the screening energy between the two environments was deduced to be $\Delta U = 235 \pm 63$ (^{6}Li+d) and 140 ± 82 eV (^{7}Li+p), although the screening energy for liquid Li has a large uncertainty with $U_{\mathrm{liq}} \sim 486$–$776$ (^{6}Li+d) and 324–637 eV (^{7}Li+p) owing to the uncertainty of the astrophysical bare $S(E)$ factors. This difference in the screening energy should be considered in such a way that, in liquid Li metal, conduction electrons and Li^{+} ions contribute to the screening in addition to bound electrons.

KEYWORDS: d-^{6}Li/p-^{7}Li reaction, modified $S^{*}(E)$ factor, electron screening, ionic screening, liquid metal target

1. Introduction

Nuclear reactions play a key role in nuclear astrophysics in clarifying the early universe and the evolution of the stars.[1)] For this reason, the cross section $\sigma(E)$ of an important astrophysical reaction at the relevant thermal energy must be known accurately. However, direct measurements of the reaction cross section between charged particles at astrophysical energies are severely hindered by the presence of the Coulomb barrier. Since the cross section $\sigma(E)$ drops steeply at an energy E far below the Coulomb barrier, it is advantageous to transform the cross section into the astrophysical $S(E)$ factor,[2)] defined as

$$\sigma(E_{\mathrm{cm}}) = S(E_{\mathrm{cm}}) E_{\mathrm{cm}}^{-1} \exp[-2\pi\eta(E_{\mathrm{cm}})], \quad (1)$$

where $\eta(E_{\mathrm{cm}}) = Z_1 Z_2 e^2/\hbar v$ is the Sommerfeld parameter (Z_1 and Z_2 are the atomic numbers of the projectile and the target nucleus, respectively, and v is the relative velocity between them) and E_{cm} is the projectile energy in the centre-of-mass (cm) system (all energies are given in the cm system in the following, except where quoted differently).

If a nuclear reaction proceeds between two bare nuclei, eq. (1) depicts a pure nuclear cross section, which we call the bare cross section (σ_{bare}), and the corresponding S-factor is called the bare S-factor [$S_{\mathrm{bare}}(E)$]. However, for reactions studied in the laboratory, the target nuclei and projectiles are usually in the form of neutral atoms, molecules, or ions. Consequently, the electron clouds surrounding the interacting nuclei screen the repulsive Coulomb potential between the bare nuclei. This leads to an enhanced cross section ($\sigma_{\mathrm{screened}}$) and a screened S-factor [$S_{\mathrm{screened}}(E)$] defined as

$$S_{\mathrm{screened}}(E) = f(E, U_{\mathrm{s}}) \cdot S_{\mathrm{bare}}(E) \ (\text{i.e., } \sigma_{\mathrm{screened}} = f \cdot \sigma_{\mathrm{bare}}). \quad (2)$$

Here, $f(E, U_{\mathrm{s}})$ is the enhancement factor[3)] defined as

$$f(E, U_{\mathrm{s}}) = \frac{E}{E + U_{\mathrm{s}}} \exp\left(\pi\eta \frac{U_{\mathrm{s}}}{E}\right) \approx \exp\left(\pi\eta \frac{U_{\mathrm{s}}}{E}\right), \quad (3)$$

where U_{s} is the screening energy provided by the environment; $f(E, U_{\mathrm{s}})$ increases exponentially as the energy decreases. The value of U_{s} due to the bound electrons can be estimated by the adiabatic limit as the difference in the electron binding energies (B_{el}) between the unified atom ($Z = Z_1 + Z_2$) and the two atoms of the entrance channel, i.e., $U_{\mathrm{s}} = B_{\mathrm{el}}(Z) - B_{\mathrm{el}}(Z_1) - B_{\mathrm{el}}(Z_2)$.[4)] This is the maximum energy transfer from bound electrons to the kinetic energy of the colliding nuclei.

For reactions with light nuclei, $S_{\mathrm{bare}}(E)$ is deduced experimentally by assuming a polynomial function of E, whose coefficients are usually determined at higher energies ($E/U_{\mathrm{s}} \gg 100$), where the screening does not affect the cross section. Then, the values of U_{s} are determined from lower-energy data so as to explain the observed enhancement. The reported values of U_{s} for bound electrons are always larger than those of the adiabatic limit. For the Li+p and Li+d reactions, Engstler *et al.*[5)] reported a screening energy of about 350 eV, which is much larger than the adiabatic limit for the Li atom (186 eV). Barker[6)] reanalyzed the data in ref. 5 so as to determine the values of U_{s} and $S_{\mathrm{bare}}(E)$ simultaneously. The obtained values were about 220 eV, which is considerably smaller than that reported in ref. 5, although still larger than 186 eV. Meanwhile, the so-called trojan horse method (THM)[7)] has been developed to deduce $S_{\mathrm{bare}}(E)$ using a quasi-free process in a three-body reaction. Using the THM, Musumarra *et al.*[8)] and Lattuada *et al.*[9)] determined $S_{\mathrm{bare}}(E)$ and obtained a U_{s} of about 320 eV by comparison with the data in ref. 5. It appears that the experimental $S_{\mathrm{bare}}(E)$ for the Li+p/Li+d reaction has not yet been determined unambiguously. In addition, the larger value of U_{s} for the bound electrons has not been explained either.

*E-mail: fangkh@lzu.edu.cn
†Present address: Institute of Material Structure Science, KEK, Tsukuba, Ibaraki 305-0801, Japan.
‡Present address: Japan Atomic Energy Agency, Tokai, Ibaraki 319-1194, Japan.
§Present address: Renesas Electronics Corporation, Kawasaki 211-8668, Japan.

Recently, it has been reported that there are surprisingly large screening effects for the D+D[10–12] and Li+p/Li+d reactions[13,14] in metal environments. In a metal, the screening due to the conduction electrons should be considered in addition to that due to the bound electrons. However, observed values of U_s for the D+D reaction are more than 300 eV for most metals, which is much larger than those predicted using the Thomas–Fermi model (several tens of eV). For the ^{6}Li(d,α)^{4}He and ^{7}Li(p,α)^{4}He reactions, the reported values of U_s are sometimes anomalously larger than 1000 eV; they are $U_s = 1500 \pm 310$ eV[13] and 3790 ± 330[14] in Pd (PdLi$_x$ target), and $U_s = 1280 \pm 60$ eV[14] in Li (solid Li metal target).

These abnormal observations have motivated us to study the screening effect due to metal environments more deeply. We have developed a liquid Li target and performed preliminary tests for the ^{6}Li+d/^{7}Li+p reactions.[15–17] In liquid Li metal, the Li ions become mobile and can contribute to the screening in addition to the electrons. Thus, a much larger screening effect is expected to be observed. However, it is inevitable that the values of U_s in liquid Li cannot be determined definitely, because the value of $S_{bare}(E)$ is unclear and confusing as already pointed out. In the present work, the analyses of data for thick-target-yield measurements have been performed. We have introduced a modified $S(E)$ factor in order to discuss the difference ($\Delta U_s^{liq\text{-}atom}$) in U_s between liquid Li and atomic/molecular Li: $\Delta U_s^{liq\text{-}atom}$ can be definitively deduced from the present data together with those in ref. 5.

2. Experimental Procedure

The experiment was performed using a low-energy high-current ion beam generator at the Laboratory of Nuclear Science of Tohoku University, details of which were reported in refs. 11, 13, and 15. Figure 1 shows the experimental setup in the present work. We used target chamber 2 for the liquid metal experiment. After passing through the target chamber 1, a proton/deuteron beam is bent by an angle of 60° with respect to the horizontal plane to enter target chamber 2. The inside of target chamber is shown in the insert of Fig. 1.

The liquid Li target was in an open container, which was placed horizontally at the center of the chamber. For the ^{6}Li(d,α)^{4}He reaction, enriched ^{6}Li (enriched to 95%) was used for the target, and natural Li (92.5% ^{7}Li) was used for the ^{7}Li(p,α)^{4}He reaction. A lump of Li was placed in the container and was heated until it melted. Then, it was kept at a temperature of approximately 250 °C; the temperature of the target was continuously monitored by an IR thermometer. The pressure in the chamber was about 4×10^{-4} Pa.

The beam spot size on the target (~5 mm diameter) was defined by an aperture at the entrance of the chamber. In order to deduce the number of projectiles, the electric current from the target was directly measured. For this purpose, two parallel magnets were fixed on opposite sides of the target; they served to restrain the secondary electron emission. The actual beam current was measured directly with a movable Faraday cup, which was inserted above the target, and was compared with the target current for various bombardment energies. The ratio between the currents

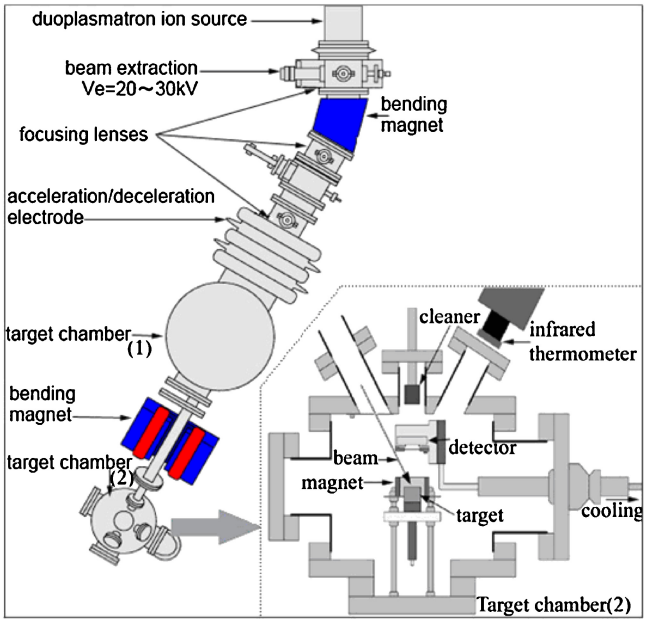

Fig. 1. (Color online) Schematic diagram of the experimental setup. The insert shows the inside of target chamber 2 used in the present work.

remained within 1%. The bombardment energy of the beam was from 22.5 to 70 keV in 2.5 keV steps. We kept the same beam power (300 mW) for each energy in order to keep as similar target conditions as possible.

A Si surface barrier detector (300 μm in thickness and 450 mm^2 in area) was employed to detect charged particles. For the ^{6}Li(d,α)^{4}He reaction, one detector was used with a solid angle ($\Delta\Omega/4\pi$) of 1.9%, and two detectors were used for the ^{7}Li(p,α)^{4}He reaction with a total solid angle of 4.5%. The detectors were placed at an angle of 125° to the beam direction. In order to prevent scattered particles from colliding with the detector directly, a thin Al foil (5 μm thick) was placed in front of the detector. The detector holder, which was made of Al, was cooled by water at 5 °C to avoid being heated up by the thermal emission from the target.

We paid close attention to the cleanness of the target surface, because Li is known to be a reactive element and is easily covered with compound materials such as LiD(H). Such deterioration clearly occurred for the liquid Li target, since the reading of the radiation thermometer fluctuated anomalously owing to the rapid motion of contaminant particles, and the yield of protons from the D(d,p)T reaction increased rapidly during the measurement of the ^{6}Li(d,α)^{4}He reaction. Thus, during the measurements, we kept the D/Li atomic ratio less than 0.5%. When the ratio exceeded the above value, the target surface was shaved by a scraper in the chamber. For the ^{7}Li(p,α)^{4}He reaction, we cleaned the surface every 2 h.

Charged particle spectra measured at 60 keV are illustrated in Figs. 2(a) and 2(b) for the ^{6}Li(d,α)^{4}He and ^{7}Li(p,α)^{4}He reactions, respectively. Four peaks are clearly seen in Fig. 2(a): they correspond to protons from the D(d,p)T reaction, protons from the ^{6}Li(d,p$_{0,1}$)^{7}Li reaction, and α-particles from the ^{6}Li(d,α)^{4}He reaction as indicated. The continuously distributed events below 1000 channels

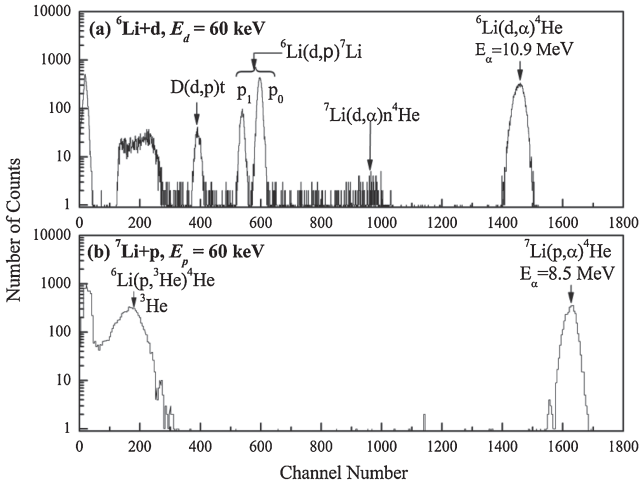

Fig. 2. Charged particle spectra obtained by the bombardment of D^+ (a) and H^+ (b) on a liquid lithium target at 60 keV.

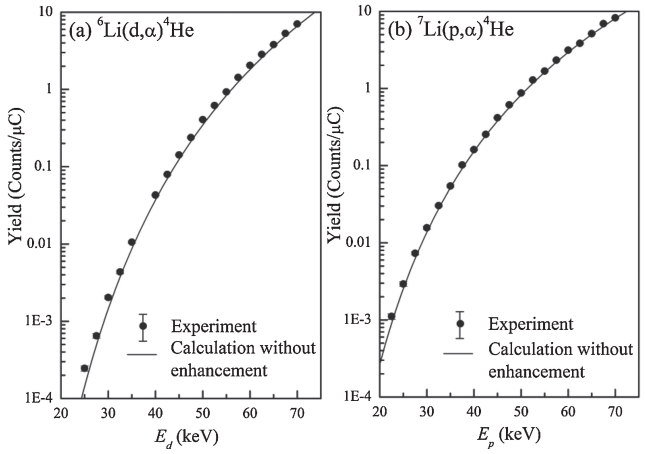

Fig. 3. Experimental thick target-yields (solid circles) of alpha particles from the ^{6}Li(d,α)^{4}He (a) and ^{7}Li(p,α)^{4}He (b) reactions. The solid curves are their corresponding calculated yields without the screening effect.

originate from the ^{7}Li(d,α)n^{4}He reaction. In Fig. 2(b), a sharp peak of α-particles from the ^{7}Li(p,α)^{4}He reaction is seen at approximately 1620 channels and the broad peak below 200 channels corresponds to ^{3}He particles from the ^{6}Li(p,^{3}He)^{4}He reaction.

3. Analysis and Results

The obtained thick-target yields $[Y_\alpha^{\rm exp}(E_{\rm lab})]$ of alpha particles from the ^{6}Li(d,α)^{4}He and ^{7}Li(p,α)^{4}He reactions are plotted in Fig. 3 (solid circles) as a function of the bombardment energy. The yields decrease exponentially as the energy decreases, since the thick-target yield is essentially an energy integral of the cross section divided by the stopping power of the beam particle: For the projectile energy $E_{\rm p}$ (in the laboratory system), it is expressed as

$$\begin{aligned} Y_\alpha^{\rm thick}(E_{\rm p}) &= 2N_{\rm p}N_{\rm t}\frac{\Delta\Omega_{\rm lab}}{4\pi}\int_0^{E_{\rm p}}\frac{{\rm d}\Omega_{\rm cm}(E_{\rm p})}{{\rm d}\Omega_{\rm lab}(E_{\rm p})}\sigma(E_{\rm cm})\left[\frac{{\rm d}E}{{\rm d}x}(E_{\rm p})\right]^{-1}{\rm d}E \\ &= 2N_{\rm p}N_{\rm t}\frac{\Delta\Omega_{\rm lab}}{4\pi}\int_0^{E_{\rm p}}\frac{{\rm d}\Omega_{\rm cm}(E_{\rm p})}{{\rm d}\Omega_{\rm lab}(E_{\rm p})}S(E_{\rm cm})E_{\rm cm}^{-1}\exp[-2\pi\eta(E_{\rm cm})]\left[\frac{{\rm d}E}{{\rm d}x}(E_{\rm p})\right]^{-1}{\rm d}E, \end{aligned} \tag{4}$$

where $N_{\rm p}$ is the number of projectiles, $N_{\rm t}$ is the number density of target atoms, $\Delta\Omega_{\rm lab}$ is the solid angle subtended by the detector, ${\rm d}\Omega_{\rm cm}/{\rm d}\Omega_{\rm lab}$ is the solid angle ratio of the cm system to the laboratory (lab) system, ${\rm d}E/{\rm d}x$ is the stopping power of lithium for incident particles, and $E_{\rm cm} = E_{\rm p} \times m_{\rm t}/(m_{\rm t} + m_{\rm p})$ is the incident energy in the cm system. The solid curves in Fig. 3 correspond to the thick-target yields calculated with the stopping power obtained from the SRIM code[18] and $S(E_{\rm cm}) = 17.8$ and 0.077. Although the calculations roughly explain the experimental yields obtained with these constant values of $S(E_{\rm cm})$, the experimental yields are slightly enhanced at low energies. These deviations from the solid curves contain information on the $S(E)$ factor and/or the screening energy for the reactions in liquid Li.

In order to compare the $S(E)$ factors in liquid Li with those for atoms/molecules as well as with the bare S-factors previously reported, we define the modified $S(E)$ factor $[S^*(E)]$ for the projectile energy $(E_{\rm cm})$ as

$$S^*(E_{\rm cm}) = \frac{\displaystyle\int_0^{E_{\rm p}}\frac{{\rm d}\Omega_{\rm cm}(E_{\rm p})}{{\rm d}\Omega_{\rm lab}(E_{\rm p})}S(E_{\rm cm})E_{\rm cm}^{-1}\exp[-2\pi\eta(E_{\rm cm})]\left[\frac{{\rm d}E}{{\rm d}x}(E_{\rm p})\right]^{-1}{\rm d}E}{\displaystyle\int_0^{E_{\rm p}}\frac{{\rm d}\Omega_{\rm cm}(E_{\rm p})}{{\rm d}\Omega_{\rm lab}(E_{\rm p})}E_{\rm cm}^{-1}\exp[-2\pi\eta(E_{\rm cm})]\left[\frac{{\rm d}E}{{\rm d}x}(E_{\rm p})\right]^{-1}{\rm d}E}, \tag{5}$$

which is about 1.8% different from the value of $S(E_{\rm cm})$ defined in eq. (1) owing to the integration in the low-energy region ($E_{\rm cm} < 60$ keV), and the difference becomes smaller as the energy decreases. The experimental $S^*(E)$, which should be compared with the calculated value, is deduced from the thick-target yields as

$$S^*_{\rm exp}(E_{\rm cm}) = \frac{Y_\alpha^{\rm exp}(E_{\rm p})}{2N_{\rm p}N_{\rm t}\dfrac{\Delta\Omega_{\rm lab}}{4\pi}\displaystyle\int_0^{E_{\rm p}}\frac{{\rm d}\Omega_{\rm cm}(E_{\rm p})}{{\rm d}\Omega_{\rm lab}(E_{\rm p})}E_{\rm cm}^{-1}\exp[-2\pi\eta(E_{\rm cm})]\left[\frac{{\rm d}E}{{\rm d}x}(E_{\rm p})\right]^{-1}{\rm d}E}. \tag{6}$$

In Figs. 4(a) and 4(b), the present results of $S^*_{\rm exp}$ are plotted with solid circles for the ^{6}Li(d,α)^{4}He and ^{7}Li(p,α)^{4}He reactions, respectively. Those of $S^*_{\rm bare}(E)$, which are deduced from the reported bare $S(E)$ factors in refs. 8 and 9, ref. 5, ref. 6, and ref. 19, are plotted with solid, dashed, dotted, and dash-dotted curves, respectively. The solid curves correspond to $S_{\rm bare}(E) = 16.9 - 41.6E + 28.2E^2$ (^{6}Li+d) and $0.055 + 0.210E - 0.310E^2$ (^{7}Li+p), the dashed curves correspond to $S_{\rm bare}(E) = 18.8 - 58.5E + 66.6E^2 - 25.8E^3$ (^{6}Li+d) and $0.0593 + 0.193E - 0.356E^2 + 0.236E^3$ (^{7}Li+p), the dotted curves correspond to $S_{\rm bare}(E) = 19.7 - 66.0E + 79.7E^2 - 33.0E^3$ (^{6}Li+d) and $0.0621 + 0.159E - 0.280E^2 + 0.186E^3$

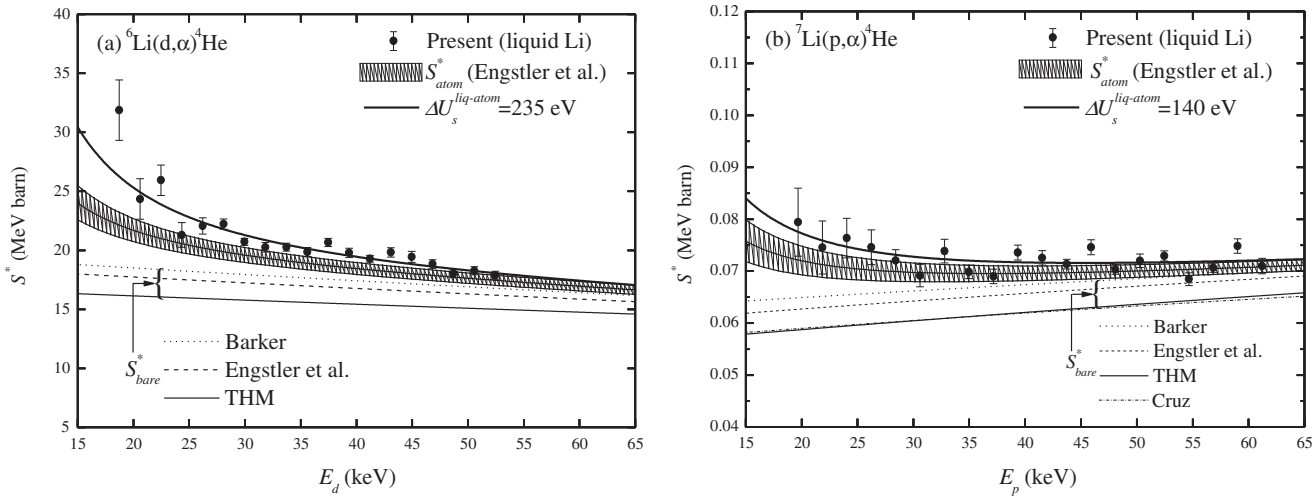

Fig. 4. $S^*(E)$ factor of the ^{6}Li(d,α)^{4}He (a) and ^{7}Li(p,α)^{4}He (b) reactions. The present result, $S^*_{liq}(E)$, is plotted with solid circles. The $S^*_{bare}(E)$ corresponding to S_{bare} are plotted with a solid line (refs. 8 and 9), a dashed line (ref. 5), a dotted line (ref. 6), and a dash-dotted line (ref. 19). The shaded regions show $S^*_{atom}(E)$ deduced by parameterization of the experimental $S(E)$ reported in ref. 5. The thick solid curve is the calculation giving the best fit to the data with $\Delta U_s^{liq\text{-}atom} = 235$ and 140 eV for (a) and (b), respectively.

(^{7}Li+p), and the dash-dotted curve corresponds to $S_{bare}(E) = 0.0556 + 0.195E - 0.451E^2 + 0.437E^3$ (^{7}Li+p, estimated from ref. 19, $E < 400$ keV). The shaded regions in Fig. 4 correspond to the experimental $S(E)$ factors for the atomic/molecular environment (S_{atom}) reported by Engstler *et al.*[5] Owing to the bound electrons, S_{atom} should involve the screening effect and take the form of eq. (2). Thus, S_{atom} is approximated as

$$\begin{aligned} S_{atom}(E) &= \exp\left[\frac{0.0142(\pm 0.0026)}{E^{3/2}}\right] \times [19.7(\pm 0.29) - 62.9(\pm 0.7)E + 79.7(\pm 1.6)E^2] \ (^6\text{Li+d}) \\ S_{atom}(E) &= \exp\left[\frac{0.0102(\pm 0.0024)}{E^{3/2}}\right] \times [0.0613(\pm 0.00072) + 0.163(\pm 0.002)E - 0.230(\pm 0.011)E^2] \ (^7\text{Li+p}). \end{aligned} \tag{7}$$

The first exponential term originates from the enhancement factor $[f(E, U_s)]$ and the second polynomial part contains the nuclear effect $[S_{bare}(E)]$ for each reaction. However, we simply treat eq. (7) as an empirical parameterization of the experimental $S_{atom}(E)$ and do not separately discuss the enhancement factor and astrophysical factor, because S_{bare} does not have to be definitively determined. The shaded regions show statistical errors (one standard deviation) estimated from the data.

As seen in Fig. 4, the values of S^*_{exp} are systematically larger than those of S^*_{atom}. This additional enhancement is caused by the stronger screening effect in the liquid metal environment than that in the atomic environment. Since various values of $S_{bare}(E)$ have been proposed, as plotted in Fig. 4, the screening energy of the ^{6}Li+d and ^{7}Li+p reactions in liquid Li cannot be determined unambiguously. Thus, we deduce the value of the screening energy difference ($\Delta U_s^{liq\text{-}atom}$) between liquid and atomic Li from the chi-square test; i.e., the value of $\Delta U_s^{liq\text{-}atom}$ is searched for that gives the minimum value of χ^2, defined as

$$\chi^2 = \sum \frac{(S^*_{exp} - S^*_{fit})^2}{(\Delta S^*_{exp})^2}, \tag{8}$$

where S^*_{fit} is expressed as

$$S^*_{fit}(E_{cm}) = \frac{\displaystyle\int_0^{E_p} \frac{d\Omega_{cm}(E_p)}{d\Omega_{lab}(E_p)} f(E_{cm}, \Delta U_s^{liq\text{-}atom}) S_{atom}(E_{cm}) E_{cm}^{-1} \exp[-2\pi\eta(E_{cm})] \left[\frac{dE}{dx}(E_p)\right]^{-1} dE}{\displaystyle\int_0^{E_p} \frac{d\Omega_{cm}(E_p)}{d\Omega_{lab}(E_p)} E_{cm}^{-1} \exp[-2\pi\eta(E_{cm})] \left[\frac{dE}{dx}(E_p)\right]^{-1} dE}. \tag{9}$$

Using the S_{atom} given in eq. (7), we obtained $\Delta U_s^{liq\text{-}atom} = 235 \pm 63$ and 140 ± 82 eV for the ^{6}Li(d,α)^{4}He and ^{7}Li(p,α)^{4}He reactions, respectively. The best fits to S^*_{exp} are plotted with thick solid curves in Fig. 4. The systematic errors of $\Delta U_s^{liq\text{-}atom}$ are estimated to be follows: ±35 eV (for $\delta\Delta\Omega$), ±35 eV (for $\delta E_{deuteron}$), and ±93 eV [for $\delta(dE/dx)$] for the ^{6}Li(d,α)^{4}He reaction, and ±58 eV (for $\delta\Delta\Omega$), ±46 eV (for δE_{proton}), and ±157 eV [for $\delta(dE/dx)$] for the ^{7}Li(p,α)^{4}He reaction.

To obtain the absolute values of the screening energy in liquid Li, we apply the same method for each S_{bare}. The deduced values of U_s are widely spread out, from 486 to 776 eV for the ^{6}Li+d reaction and from 324 to 637 eV for the ^{7}Li+p reaction. The smallest values correspond to the S_{bare} obtained by Barker,[6] while the largest ones correspond to that obtained by the THM.[8,9] Therefore, it is concluded that the present work gives definitive values of $\Delta U_s^{liq\text{-}atom}$, although the values of U_{liq} contain large uncertainties.

4. Discussion

In a simple picture, the screened Coulomb potential (ϕ_s) of a Li nucleus is given by the bare Coulomb potential multiplied by an exponential screened function as

$$\phi_s(r) = \frac{3e}{r}\exp\left(-\frac{r}{D_s}\right) \approx \frac{3e}{r} - \frac{3e}{D_s}, \qquad (10)$$

where e is the elementary charge and D_s is called the screening length. Thus, the screening energy between a Li nucleus and a proton (or deuteron) U_s is $U_s = 3e^2/D_s$. Since the electrons and ions surrounding the target nucleus can contribute to the screening of the Coulomb potential in liquid metal Li, the origins of the screening energy (U_{liq}) in liquid Li are considered to be the bound electrons (U_{be}) of Li atoms or Li compounds, conduction electrons (U_{ce}), and Li^+ ions (U_{ion}). Thus, D_{liq} is given by $1/D_{liq}^2 = 1/D_{be}^2 + 1/D_{ce}^2 + 1/D_{ion}^2$ or $U_{liq}^2 = U_{be}^2 + U_{ce}^2 + U_{ion}^2$. On the other hand, only the bound electrons can contribute to the screening energy for a Li nucleus in the atomic/molecular environment. Therefore, the $\Delta U_s^{liq\text{-}atom}$ deduced in the present work can be expressed in terms of the contributions from the conduction electrons and Li ions as $(\Delta U_s^{liq\text{-}atom})^2 = (U_{ce})^2 + (U_{ion})^2$.

The value of U_{ce} is estimated from the Thomas–Fermi screening model,[20] which predicts that $D_{ce} = (6\pi e^2 N_e/E_F)^{-1/2}$, where N_e is the number density of conduction electrons and E_F is the Fermi energy of an electron. Using $N_e \approx N_{Li} = 4.7 \times 10^{22}\,cm^{-3}$ and $E_F = 4.7\,eV$, we obtain $U_{ce} = 71\,eV$. Since the Li^+ ions in liquid lithium can be treated as classical particles, U_{ion} is estimated by Debye screening,[21] which gives $U_{Debye} = 3e^2(4\pi e^2 N_{Li}/kT)^{1/2}$ for lithium number density N_{Li}, Boltzmann constant k, and temperature T. Using the experimental conditions $N_{Li} = 4.7 \times 10^{22}\,cm^{-3}$ and $T = 520\,K$, we obtain $U_{ion} = 593\,eV$. Therefore, the estimated value of $\Delta U_s^{liq\text{-}atom}$ is 598 eV, which is much larger than the experimental results; more than 360 and 460 eV larger, respectively, than the results for the $^6Li(d,\alpha)^4He$ and $^7Li(p,\alpha)^4He$ reactions. Since the main part of the predicted $\Delta U_s^{liq\text{-}atom}$ originates from the Li ions, the simple application of the Debye screening model to the ionic screening in liquid Li cannot be justified. One may argue that the Debye model can be applied only for weakly coupled plasmas, but liquid Li is classified as a strongly coupled plasma. Although a more sophisticated calculation that includes the effect of the interaction between the Li ions is required, we can claim that the screening energy originating from the Li ions is much smaller than that predicted by the simple Debye model. In order to explain the experimental value of $\Delta U_s^{liq\text{-}atom}$, a reduction factor ($R$) is needed as $U_{ion} = R \times U_{debye}$, $R = 0.2$–0.4. Since the mass of ions is much larger than that of electrons, the Li^+ ions cannot respond quickly; this results in a weakening of the ionic screening effect.

It was reported by Cruz *et al.*[14] that the $^7Li(p,\alpha)^4He$ reaction in solid Li metal gives a very large screening energy of $U_{sol} = 1280 \pm 60\,eV$, which is more than 2 times larger than the largest value of U_{liq} (corresponding to the S_{bare} reported in ref. 9). If we estimate the screening energy originating from ions using Cruz *et al.*'s U_{sol} together with the presently deduced U_{liq}, then the ionic screening potential should be about $-1100\,eV$ (antiscreening). It appears to be almost impossible to predict such a large antiscreening due to ions. Thus, it is very difficult to understand the anomalously large value of U_{sol} reported in ref. 14. However, in our experience, the solid Li target is more easily deteriorated/contaminated chemically and the stopping power becomes larger than that expected for pure Li metal. As Cruz *et al.*[14] discussed in their article, the solid Li target had a dark color at the beam spot area, which might indicate that its surface was seriously contaminated. Note that a larger value of $S(E)$ is deduced when the stopping power is underestimated.

In the Pd metal environment, huge values of the screening energy were also reported for the ^6Li+d[13] and ^7Li+p[14] reactions. These values are anomalously large but do not agree with each other ($1500 \pm 310\,eV$[13] and $3790 \pm 330\,eV$[14]). As discussed above, the origins of the screening effect might be the bound electrons of Li atoms, conduction electrons, and ions. Even if both the electrons ($U_{be} = 186\,eV$ and $U_{ce} = 71\,eV$) and ions (if they exist, $U_{ion} = 593\,eV$) fully contribute to the screening in liquid Li, a screening energy larger than 700 eV cannot be expected. This, together with the large difference between the two results, suggests that experimental problems still exist. The most difficult issue in this type of experiment is to determine the number of target Li near the surface of the metal foil, where the reaction mainly occurs.

5. Summary and Conclusions

The reactions $^6Li(d,\alpha)^4He$ and $^7Li(p,\alpha)^4He$ have been studied in liquid metal Li, for the first time, at bombardment energies between 22.5 and 70 keV. The excitation function of the thick-target yield of α particles has been measured while keeping the surface of the liquid Li target as clean as possible. The modified $S(E)$ factors in liquid Li deduced from the present data are compared with those of S_{atom} and S_{bare}. The comparison shows a clear difference in the S factors for different environments; i.e., $S^*_{liq} > S^*_{atomic} > S^*_{bare}$.

Since S_{bare} is not determined unambiguously, the screening energy difference between liquid Li and atomic/molecular Li is obtained as $\Delta U_s^{liq\text{-}atom} = 235 \pm 63$ and $140 \pm 82\,eV$ for the $^6Li(d,\alpha)^4He$ and $^7Li(p,\alpha)^4He$ reactions, respectively. This additional screening energy provided by the liquid metal environment is considered to be caused by the conduction electrons as well as free Li^+ ions. The screening energies are estimated simply by the Thomas–Fermi model for the conduction electrons and by the Debye model for the Li ions. It turns out that ionic screening is suppressed to about 40% of the value predicted by the simple Debye model. Although the model might not be applicable to liquid Li, the suppression of ionic screening may be due to the heavy mass of the ions, which cannot respond quickly. For electronic screening, it is highly desirable to determine the value of S_{bare} experimentally. The screening energy for solid Li is also required.

We conclude that the existence of both electronic and ionic screening in liquid Li metal enhanced the reaction rate of low-energy nuclear reactions, although the screening potential difference is not reproduced by the simple predictions of Debye screening and the Thomas–Fermi model. It is highly desirable to develop a more sophisticated theory for the screening mechanism in liquid metal Li.

Acknowledgments

K. H. Fang and T. S. Wang thank Tohoku University for their hospitality during the experiments and J. Kasagi thanks the hospitality of Lanzhou University during the analyses. This work was partly supported by a Grant-in-Aid for Scientific Research (No. 19340051) from the Ministry of Education, Culture, Sports, Science and Technology of Japan and the National Natural Science Foundation of China (No. 10675056).

1) W. A. Fowler: Rev. Mod. Phys. **56** (1984) 149.
2) C. Rolfs and W. W. Rodney: *Cauldrons in the Cosmos* (University of Chicago Press, Chicago, IL, 1988).
3) H. J. Assenbaum, K. Langanke, and C. Rolfs: Z. Phys. A **327** (1987) 461.
4) L. Bracci, G. Fiorentini, V. S. Melezhik, G. Mezzorani, and P. Quarati: Nucl. Phys. A **513** (1990) 316.
5) S. Engstler, G. Raimann, C. Angulo, U. Greife, C. Rolfs, U. Schroder, E. Somorjai, B. Kirch, and K. Langanke: Z. Phys. A **342** (1992) 471.
6) F. C. Barker: Nucl. Phys. A **707** (2002) 277.
7) G. Baur: Phys. Lett. B **178** (1986) 135.
8) A. Musumarra, R. G. Pizzone, S. Blagus, M. Bogovac, P. Figuera, M. Lattuada, M. Milin, D. Miljanic, M. G. Pellegriti, D. Rendic, C. Rolfs, N. Soic, C. Spitaleri, S. Typel, H. H. Wolter, and M. Zadro: Phys. Rev. C **64** (2001) 068801.
9) M. Lattuada, R. G. Pizzone, S. Typel, P. Figuera, A. Miljanic, A. Musumarra, M. G. Pellegriti, C. Rolfs, C. Spitaleri, and H. H. Wolter: Astrophys. J. **562** (2001) 1076.
10) K. Czerski, A. Huke, A. Biller, P. Heide, M. Hoeft, and G. Ruprecht: Europhys. Lett. **54** (2001) 449.
11) H. Yuki, J. Kasagi, A. G. Lipson, T. Ohtsuki, T. Baba, T. Noda, B. F. Lyakhov, and N. Asami: JETP Lett. **68** (1998) 823.
12) F. Raiola, L. Gang, C. Bonomo, G. Gyürky, M. Aliotta, H. W. Becker, R. Bonetti, C. Broggini, P. Corvisiero, A. D'Onofrio, Z. Fülöp, G. Gervino, L. Gialanella, M. Junker, P. Prati, V. Roca, C. Rolfs, M. Romano, E. Somorjai, F. Strieder, F. Terrasi, G. Fiorentini, K. Langanke, and J. Winter: Eur. Phys. J. A **19** (2004) 283.
13) J. Kasagi, H. Yuki, T. Baba, T. Noda, J. Taguchi, M. Shimokawa, and W. Galster: J. Phys. Soc. Jpn. **73** (2004) 608.
14) J. Cruz, Z. Fulop, G. Gyurky, F. Raiola, A. D. Leva, B. Limata, M. Fonseca, H. Luis, D. Schurmann, M. Aliotta, H. W. Becker, A. P. Jesus, K. U. Kettner, J. P. Ribeiro, C. Rolfs, M. Romano, E. Somorjai, and F. Strieder: Phys. Lett. B **624** (2005) 181.
15) H. Yonemura, J. Kasagi, M. Honmo, Y. Ishikawa, T. Wang, and Y. Zhang: AIP Conf. Proc. **853** (2006) 372.
16) J. Kasagi, H. Yonemura, Y. Toriyabe, A. Nakagawa, and T. Sugawara: AIP Conf. Proc. **1016** (2008) 233.
17) J. Kasagi and H. Yonemura: AIP Conf. Proc. **1098** (2009) 161.
18) J. F. Ziegler and J. P. Biersack: SRIM code [http://www.srim.org].
19) J. Cruz, H. Luis, M. Fonseca, Z. Fülöp, G. Gyürky, F. Raiola, M. Aliotta, K. U. Kettner, A. P. Jesus, J. P. Ribeiro, F. C. Barker, and C. Rolfs: J. Phys. G **35** (2008) 014004.
20) C. Kittel: *Introduction to Solid State Physics* (Wiley, New York, 1986) 6th ed.
21) P. Debye: *Polar Molecules* (Dover, New York, 1929).